IEEE Access
Multidisciplinary | Rapid Review | Open Access Journal

Received April 21, 2020, accepted April 29, 2020, date of publication May 6, 2020, date of current version May 18, 2020.

Digital Object Identifier 10.1109/ACCESS.2020.2992709

Generation of Antifractals via Hybrid Picard-Mann Iteration

WEI WANG[1], XIAOHUI HU[2], ABDUL AZIZ SHAHID[3], AND MINGYE WANG[1]

[1]College of Automation Science and Electrical Engineering, Beihang University, Beijing 100191, China
[2]Institute of Software, Chinese Academy of Sciences, Beijing 100190, China
[3]Department of Mathematics and Statistics, The University of Lahore, Lahore 54000, Pakistan

Corresponding author: Wei Wang (ww56050006ww@aliyun.com)

This work was supported in part by the Key Project of NSFC-Big Data Method and Solution for Complex Information under Grant U143520.

ABSTRACT The aim of this paper is to generate antifractals using fixed point iterative algorithms, i.e., we aim to generate anti Julia sets, tricorns and multicorns for the anti-polynomial $z \to \bar{z}^k + c$ of the complex polynomial $z^k + c$, for $k \geq 2$. A hybrid Picard-Mann iterative procedure used to establish escape criterion and explore the geometry of antifractals. A visualization of the antifractals for certain complex antipolynomials is presented and their graphical behavior is compared with antifratals generated via Mann iteration. We also explain the effects of parameters on shape of antifractals.

INDEX TERMS Antifractals, fixed point iterative schemes, escape criterion, tricorns and multicorns.

I. INTRODUCTION

The branch of mathematics known as fixed point theory is a powerful tool to study natural phenomena that are usually nonlinear and has many applications in almost every area of research including biology, computer sciences, image generations, complex graphics, etc [1], [2]. Fractal and antifractal images can be generated by using iterative algorithms for finding fixed points of particular mappings [1]. Very first time, Julia in the year 1918 [3] studied graphics of the following complex function (1) and lead the foundation of Fractal geometry:

$$z_{n+1} = z_n^2 + c, \tag{1}$$

where $z \in C$ and c is a fixed complex number. Later this complex set named as Julia set, which is the classical example of Fractal.

Definition 1 ([4]): Let us consider a complex valued polynomial $f : C \longrightarrow C$ with degree ≥ 2. Then the set of complex numbers F_f whose orbits does not converge to infinity is known as filled Julia set of f. Mathematically the filled Julia set is:

$$F_f = \{x \in C : \{|f^n(x)|\}_{n=0}^{\infty} \text{ is bounded } \}.$$

The Julia set is denoted by $J(f_c)$ and is the boundary of filled Julia set F_f and the complement of Julia set is called Fatou set [5].

The word Fractal was introduced by Mandelbrot and introduced Mandelbrot set [6]. He took c as a complex variable in (1) and utilized the idea of Gostan Julia to observe the behaviour of Julia sets that are connected sets [6]. Fractals don't have a conventional definition, anyway they are distinguished through their irregular structure that can't be found in Euclidean geometry.

Definition 2 ([7]): For the complex polynomial $Q_c(z) = z^2 + c$, the Mandelbrot set is the collection of all c for which the orbit of 0 is bounded and is denoted by M. Mathematical, we can write

$$M = \{c \in C : \{Q_c^n(0)\}; n = 0, 1, 2, \ldots \text{is bounded}\}.$$

The 0 has been taken as initial point because it is the only critical point for Q_c.

The Julia sets and Mandelbrot sets are the fundamental sets in fractal geometry and got special place in fractal art [8]. These sets are most complex sets till the date and can not be seen without computer [9]. There are many ways to generate Fractals and fixed point theory is one of them in which iterative algorithms are used to find fixed point of complex polynomials [10], [11]. Different researcher used different iterative algorithms to generate Fractals, for example, see [10]–[14]. Generation of Fractals is an aesthetic endeavor,

The associate editor coordinating the review of this manuscript and approving it for publication was Haiyong Zheng.

a sooting diversion or only a numerical model and fractal art is totally different from other computer activities [15].

In [16], Crowe *et al.*, first time studied the connected locus and dynamics of the quadratic antiholomorphic polynomials $\bar{z}^2 + c$ and this connected locus is called "tricorn" by Milnor in [17].

Tricorn, being a complex subset of complex numbers, plays an important role in quadratic and cubic polynomials and very much similar with Mandelbrot set. The nature of tricorn is three-cornered and the style of its self similarity exactly same as that of Mandelbrot set. In the year 1983, Crowe with his coauthors [16] studied the relationship between tricorn and Mandelbrot set, named it "Mandelbar sets" and proved that the features bifurcations of tricorn is along arcs rather than at points. Later in [18], Winters proved that the boundary of tricorn contains a smooth arc and in [19], Lau and Schleicher investigated symmetries of tricorn and multicorn. In continuation of these works, the tricorn set is generalized and multicorn set has been introduced [20]. In fact multicorns is the generalization of tericorns or multicorn set is a tricorn set of higher order. Moreover they proved that the Julia set of mapping $A_c(z) = \bar{z}^k + c$ for $k \geq 2$ is either connected or disconnected. Now we define the multicorn sets.

Definition 3 ([7]): Let us consider the mapping $A_c(z) = \bar{z}^k + c$ for $k \geq 2$. The multicorn det is denoted by M_c^* which is the collection of all complex numbers c for which the orbit of 0 is bounded. Mathematical, we can write as:

$$M_c^* = \{c \in C : A_c^n(0) \text{ does not tend to } \infty\},$$

where A_c^n is the nth iterate of the function $A_c(z)$.

In the above definition, if we take $k = 2$, multicorn set become tricorn set. In literature, one can find many ways to generate antifractals and one way is to use iterative algorithms for finding fixed point of mappings. The aim of this paper is to generate antifractals by using Picard-Mann iterative algorithm. For a complex valued mapping $T : C \to C$, the Picard orbit (PO) is defined as [21]:

$$x_{n+1} = T(x_n) \tag{2}$$

where $n \geq 0$. The Mann orbit (MO) is defined as [22]:

$$\begin{cases} x_0 \in C, \\ x_{n+1} = (1-\theta)x_n + \theta T x_n, \quad n \geq 0, \end{cases} \tag{3}$$

where $\theta \in (0, 1]$.

This is one step iterative algorithm and antifractals via MO process were studied by Rani in [23], [24]. Many authors studied the dynamical behaviour of antiholomorphic complex mappings and various fixed point iterative algorithms were utilized [25]–[27].

The following two-step Ishikawa iteration process [28] is used in [25] to generate tricorns and multicorns:

$$\begin{cases} x_0 \in C, \\ x_{n+1} = (1-\theta)x_n + \theta T y_n, \\ y_n = (1-\delta)x_n + \delta T x_n, \quad n \geq 0, \end{cases} \tag{4}$$

where θ and $\delta \in (0, 1]$.

Kwun *et al.* [29] and Chen *et al.* [30] explored tricorns and multicorns via Noor iteration with s-convexity and modified S-iteration respectively. Kang *et al.* [31] visualized tricorns and multicorns by using following S-iteration process [32]:

$$\begin{cases} x_0 \in C, \\ x_{n+1} = (1-\theta)Tx_n + \theta T y_n, \\ y_n = (1-\delta)x_n + \delta T x_n, \quad n \geq 0, \end{cases} \tag{5}$$

where θ and $\delta \in (0, 1]$.

Recently, Li *et al.* [33] introduced the antifractals by utilizing CR-iteration with s-convexity. It is seen that for each iterative process the behaviour and dynamics of the tricorn and multicorns differ. Now we define the Picard-Mann orbit (PMO) [34].

Definition 4: Consider the mapping $f : C \to C$, where C is a subset of complex plane. Then the PMO is the following sequence of iterates with initial guess $x_0 \in C$

$$\begin{cases} x_{n+1} = f(y_n), \\ y_n = (1-\theta)x_n + \theta f(x_n); \quad n \geq 0, \end{cases} \tag{6}$$

where $0 < \theta \leq 1$.

The PMO is a function of three variables (f, x_0, θ) which can be written as $PMO(f, x_0, \theta_n)$.
Khan in [34] proved that the PMO converges faster than PO, MO and Ishikawa iteration process.

Now, for polynomial $Q_c(z_n)$ of any degree, we have following PM scheme:

$$\begin{cases} z_{n+1} = Q_c(u_n), \\ u_n = (1-\theta)z_n + \theta Q_c(z_n), \quad n \geq 0, \end{cases} \tag{7}$$

where $\theta \in (0, 1]$.

In this paper we consider the iteration process of unicritical antiholomorphic polynomials $f_c(z) = \bar{z}^k + c$, for any degree $k \geq 2$ and $c \in C$ via PMO and attained diverse graphical patterns of tricorn, multicorn and anti-Julia sets that are totally different from those generated by using MO.

II. ESCAPE CRITERION FOR ANTIFRACTALS

Many techniques are used to generate and analyze fractals, such as iterated function systems, random fractals, escape time fractals etc. The escape time algorithm depends on the maximum number of iterations necessary to measure if the orbit sequence tends to infinity or not. This algorithm gives a useful mechanism applied to demonstrate some features of dynamic system under iterative procedure. Usually, the escape criterion for fractal sets is:

Theorem 1 ([7]): Let $Q_c(z) = z^2 + c$ where $c \in C$. Also let $n \geq 0$ and

$$\left|Q_c^n(z)\right| > \max\{|c|, 2\},$$

then $\left|Q_c^n(z)\right| \to \infty$ as $n \to \infty$

Here $\max\{|c|, 2\}$ is called escape radius threshold which may be different for different iterative processes. Now we obtain a general escape criterion that is necessary to construct

the antifractals for antipolynomials of the form $Q_c(z) = \overline{z}^k + c, k \geq 2$ in PMO.

Theorem 2: Let $|z| \geq |c| > (\frac{2}{\theta})^{\frac{1}{k-1}}$ *with* $k \geq 2, 0 < \theta \leq 1$ *and* c *be a complex number. Let* $z_\circ = z$ *and* $u_\circ = u$. *Define*

$$\begin{cases} z_{n+1} = Q_c(\overline{u}_n) \\ u_n = (1-\theta)z_n + \theta Q_c(\overline{z}_n), \quad n \geq 0. \end{cases}$$

Then $|z_n| \to \infty$ *as* $n \to \infty$.

Proof: For $Q_c(\overline{z}) = \overline{z}^k + c$

$$\begin{aligned} |u| &= |(1-\theta)z + \theta Q_c(\overline{z})| \\ &= \left|(1-\theta)z + \theta(\overline{z}^k + c)\right| \\ &\geq \left|\theta\overline{z}^k + (1-\theta)z\right| - |\theta c| \\ &\geq \left|\theta\overline{z}^k\right| - |(1-\theta)z| - |\theta z| \because |z| \geq |c| \\ &\geq \theta\left|\overline{z}^k\right| - |z| + |\theta z| - |\theta z| \\ &\geq |\overline{z}|\,(\theta\,|\overline{z}|^{k-1} - 1). \end{aligned}$$

Also for

$$\begin{aligned} |z_1| &= |Q_c(\overline{u})| \\ &= \left|\overline{u}^k + c\right| \\ &\geq \left|(|\overline{\overline{z}}|\,(\theta\ |\overline{\overline{z}}|^{k-1} - 1))^k + c\right| \\ &\geq \left|(|z|\,(\theta\ |z|^{k-1} - 1))^k\right| - |c| \because |\overline{\overline{z}}| = |z| \\ &\geq (|z|\,(\theta\ |z|^{k-1} - 1))^k - |z| \because |z| \geq |c| \end{aligned} \tag{8}$$

As $|z| \geq |c| > (\frac{2}{\theta})^{\frac{1}{k-1}}$ so

$$\begin{aligned} \theta\ |z|^{k-1} - 1 &\geq 1 \\ (\theta\,|z|^{k-1} - 1)^k &\geq 1 \\ |z|^k\,(\theta\,|z|^{k-1} - 1)^k &\geq |z|^k \end{aligned} \tag{9}$$

Putting in (8), we have

$$\begin{aligned} |z_1| &\geq |z|^k - |z| \\ &= |z|\,(|z|^{k-1} - 1) \end{aligned}$$

Since $|z| > (\frac{2}{\theta})^{\frac{1}{k-1}} > 2^{\frac{1}{k-1}}$ so $|z|^{k-1} - 1 > 1$. Hence we have $\mu > 0$, for which $|z|^{k-1} - 1 > 1 + \mu > 1$. Consequently

$$|z_1| \geq (1+\mu)\,|z|\,.$$

Repeatedly applying same argument, we get

$$\begin{aligned} |z_2| &\geq (1+\mu)^2\,|z|\,, \\ &\vdots \\ |z_n| &\geq (1+\mu)^n\,|z|\,. \end{aligned}$$

Hence $|z_n| \to \infty$ as $n \to \infty$. □

Now, we can get following escape criterion immediatly.

Corollary 1: If $|z| > \max\left\{|c|\,, \left(\frac{2}{\theta}\right)^{\frac{1}{k-1}}\right\}$ *then* $|z_n| \to \infty$ *as* $n \to \infty$.

Algorithm 1 Visualization of Multicorn and Tricorn

Input: $Q_c(\overline{z}) = \overline{z}^k + c$, where $c \in \mathbb{C}$ and $k \geq 2$, $A \subset \mathbb{C}$ – area, K – iterations, $\theta \in (0, 1]$ – parameter for the PMO, *colourmap*$[0..M-1]$ – with M colours.

Output: Tricorn or multicorn for A.

```
for c ∈ A do
    R = max{|c|, (2/θ)^{1/k−1}}
    n = 0
    z_0 = 0
    while n ≤ K do
        u_n = (1 − θ)z_n + θQ_c(z_n),
        z_{n+1} = Q_c(u_n)
        if |z_{n+1}| > R then
            break
        n = n + 1
    i = ⌊(M − 1)n/K⌋
    colour c with colourmap[i]
```

III. VISUALIZATION OF ANTIFRACTALS

In this section antifractals like anti-Julia sets, tricorns and multicorns are visulized for $Q_c(\overline{z}) = \overline{z}^k + c, k \geq 2$ via MO and PMO by arranging escape time algorithm for visualization of antifractals with the help of software Mathematica 9.0.

Algorithm 1 demonstrates pseudocode for the multicorns and tricorns, whereas the pseudocode for the anti-Julia set is the Algorithm 2.

Algorithm 2 Visualization of Anti-Julia Set

Input: $Q_c(\overline{z}) = \overline{z}^k + c$, where $c \in \mathbb{C}$ and $k \geq 2$, $A \subset \mathbb{C}$ – area, K – iterations, $\theta \in (0, 1]$ – parameter for the PMO, *colourmap*$[0..M-1]$ – with M colours.

Output: Anti-Julia set for A.

```
R = max{|c|, (2/θ)^{1/m−1}}
for z_0 ∈ A do
    n = 0
    while n ≤ K do
        w_n = (1 − θ)z_n + θQ_c(z̄_n),
        z_{n+1} = Q_c(w̄_n)
        if |z_{n+1}| > R then
            break
        n = n + 1
    i = ⌊(M − 1)n/K⌋
    colour z_0 with colourmap[i]
```

A. TRICORNS FOR THE FUNCTION $Q_c(\overline{z}) = \overline{z}^2 + c$

In Fig. 1 tricorn is generated in PO whereas in Figs. 2–5 and in Figs. 6–9, tricorns are visualized for quadratic function $z \to$

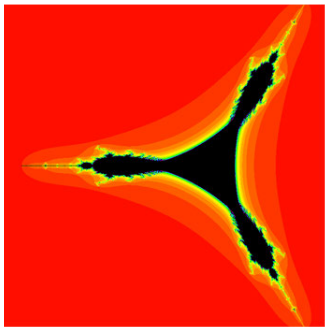

FIGURE 1. Tricorn generated via PO.

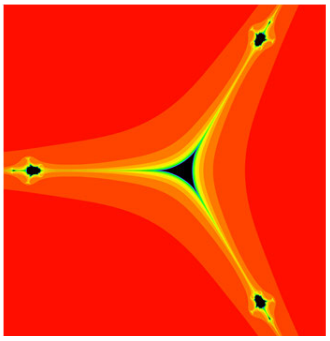

FIGURE 2. Tricorn generated via PMO for $\theta = 0.2$.

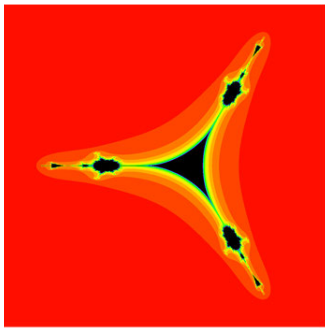

FIGURE 3. Tricorn generated via PMO for $\theta = 0.6$.

$\bar{z}^2 + c$ in PMO and MO respectively. The maximum number of iterations are fixed at 30.

- Fig. 1 $A = [-2.2, 1.2] \times [-1.7, 1.7]$.
- In Fig. 2 with $A = [-6, 4.7] \times [-5.5, 5.5]$ tricorn generated in PMO and in Fig. 6 with $A = [-6, 4.7] \times [-5.5, 5.5]$ tricorn generated in MO for same value $\theta = 0.2$.
- In Fig. 3 and Fig. 7 tricorn generated in PMO and MO respectively for $\theta = 0.6, A = [-3.7, 2.7] \times [-3.2, 3.2]$.
- In Fig. 4 and Fig. 8 tricorn obtained in PMO and MO respectively for $\theta = 0.35, A = [-6, 4.7] \times [-5.5, 5.5]$.
- In Fig. 5 with $A = [-4.4, 3.4] \times [-3.9, 3.9]$ tricorn generated in PMO and in Fig. 9 with $A = [-6, 4.7] \times [-5.5, 5.5]$ tricorn generated in MO for same value $\theta = 0.06$.

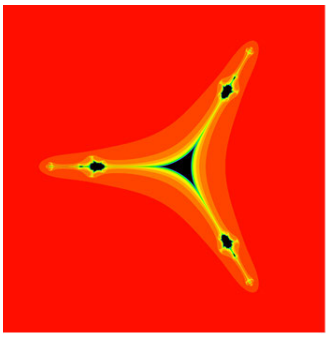

FIGURE 4. Tricorn generated via PMO for $\theta = 0.35$.

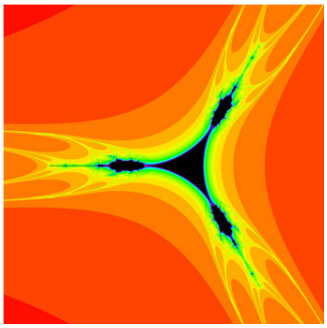

FIGURE 5. Tricorn generated via PMO for $\theta = 0.06$.

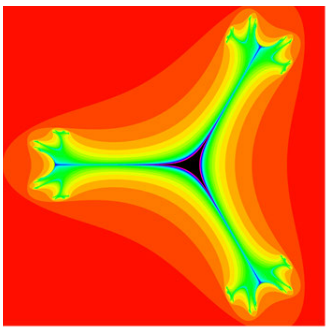

FIGURE 6. Tricorn generated via MO for $\theta = 0.2$.

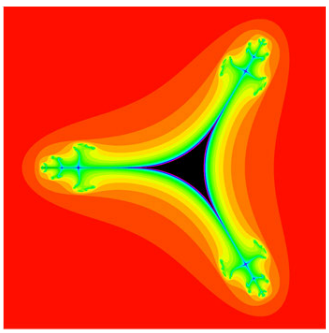

FIGURE 7. Tricorn generated via MO for $\theta = 0.6$.

B. MULTICORNS FOR THE FUNCTION $Q_c(\bar{z}) = \bar{z}^3 + c$

Multicorns are visualized for cubic function $Q_c(\bar{z}) = \bar{z}^3 + c$ via PMO in Figs. 11–14 and MO in Figs. 15–18 by choosing $K = 30$ and varying parameters as:

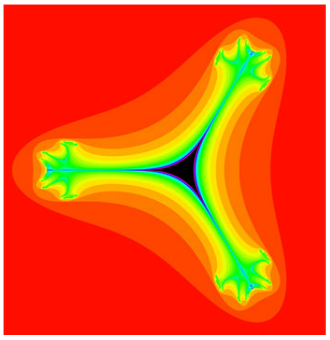

FIGURE 8. Tricorn generated via MO for $\theta = 0.35$.

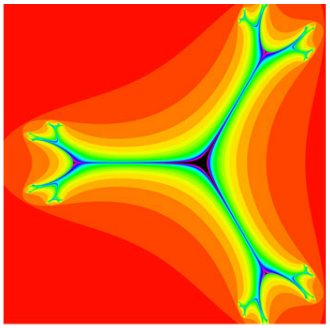

FIGURE 9. Tricorn generated via MO for $\theta = 0.06$.

FIGURE 10. Multicorn generated via PO for $k = 3$.

- Fig. 10 $A = [-1.7, 1.7] \times [-1.7, 1.7]$,
- In Fig. 11 and in Fig. 15 multicorns are generated via PMO with $\theta = 0.3, A = [-2, 2] \times [-2, 2]$.
- In Fig. 12 with $A = [-4, 4] \times [-4, 4]$ and in Fig. 16 with $A = [-6, 6] \times [-6, 6]$ multicorns are generated via PMO and MO for same value of $\theta = 0.04$.
- In Fig. 13 with $A = [-3.5, 3.5] \times [-3.5, 3.5]$ and in Fig. 17 with $A = [-5.5, 5.5] \times [-5.5, 5.5]$ multicorns are visualized via PMO and MO for same value of $\theta = 0.06$.
- In Fig. 14 with $A = [-3.2, 3.2] \times [-3.2, 3.2]$ and in Fig. 18 with $A = [-5.2, 5.2] \times [-5.2, 5.2]$ multicorns are presented in PMO and MO for similar value of $\theta = 0.08$ respectively.

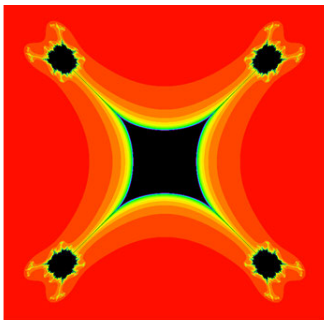

FIGURE 11. Multicorn generated via PMO for $\theta = 0.3$ and $k = 3$.

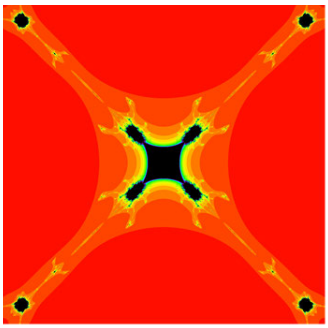

FIGURE 12. Multicorn generated via PMO for $\theta = 0.04$ and $k = 3$.

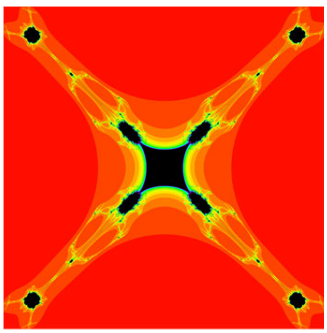

FIGURE 13. Multicorn generated via PMO for $\theta = 0.06$ and $k = 3$.

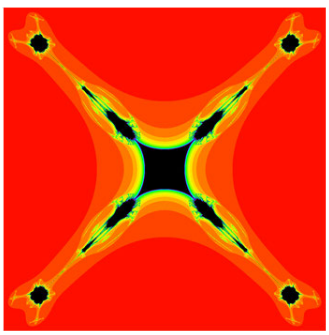

FIGURE 14. Multicorn generated via PMO for $\theta = 0.08$ and $k = 3$.

C. MULTICORNS FOR HIGHER DEGREE FUNCTIONS

Multicorns are visualized for $Q_c(\overline{z}) = \overline{z}^k + c, k \geq 4$ in PMO in Figs. 19–24 and MO in Figs. 25–30 by fixing $K = 30$ and choosing varying parameters as:

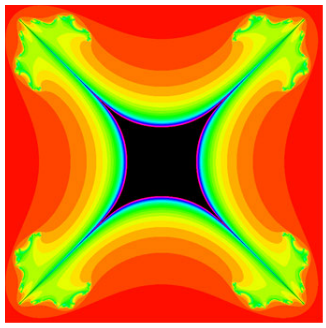

FIGURE 15. Multicorn generated via MO for $\theta = 0.3$ and $k = 3$.

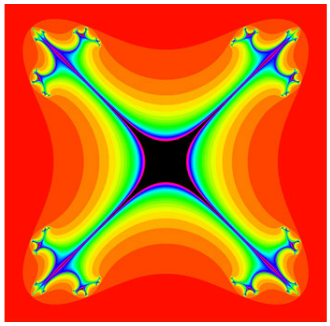

FIGURE 16. Multicorn generated via MO for $\theta = 0.04$ and $k = 3$.

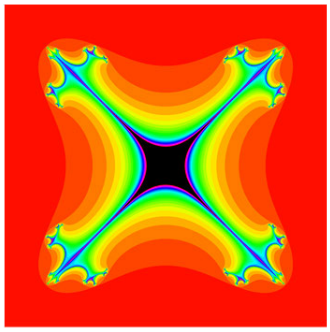

FIGURE 17. Multicorn generated via MO for $\theta = 0.06$ and $k = 3$.

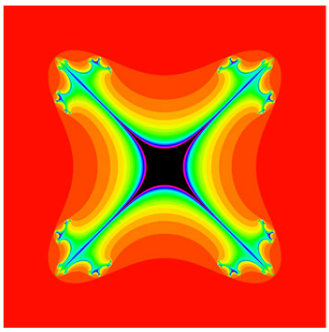

FIGURE 18. Multicorn generated via MO for $\theta = 0.08$ and $k = 3$.

- Fig. 19 generated via PMO and Fig. 25 generated via MO for $\theta = 0.5, A = [-2.2, 2.2] \times [-2.2, 2.2]$ and $k = 4$,

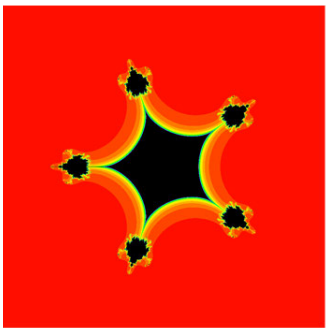

FIGURE 19. Multicorn generated via PMO for $\theta = 0.5$ and $k = 4$.

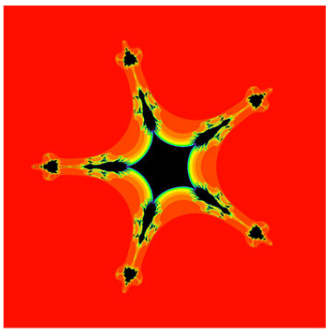

FIGURE 20. Multicorn generated via PMO for $\theta = 0.07$ and $k = 4$.

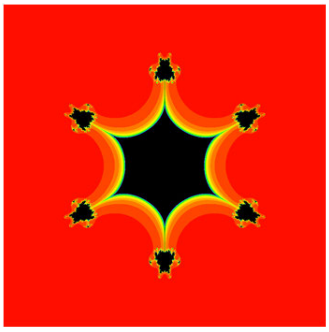

FIGURE 21. Multicorn generated via PMO for $\theta = 0.3$ and $k = 5$.

- Fig. 20 generated via PNO and Fig. 26 generated via MO for $\theta = 0.07, A = [-3.4, 3.4] \times [-3.4, 3.4]$ and $k = 4$,
- Fig. 21 generated via PMO and Fig. 27 generated via MO for $\theta = 0.3, A = [-2.2, 2.2] \times [-2.2, 2.2]$ and $k = 5$,
- Fig. 22 generated via PMO and Fig. 28 generated via MO for $\theta = 0.05, A = [-2.5, 2.5] \times [-2.5, 2.5]$ and $k = 5$,
- Fig. 23 generated via PMO and Fig. 29 generated via MO for $\theta = 0.2, A = [-2.2, 2.2] \times [-2.2, 2.2]$ and $k = 7$,
- Fig. 24 generated via PMO and Fig. 30generated via MO for $\theta = 0.4, A = [-2.0, 2.0] \times [-2.0, 2.0]$ and $k = 8$.

It is observed that tricorns and multicorns generated via PMO and MO presented in Figs. 2–30, maintain symmetry along x-axis when k is even and when k is odd the symmetry

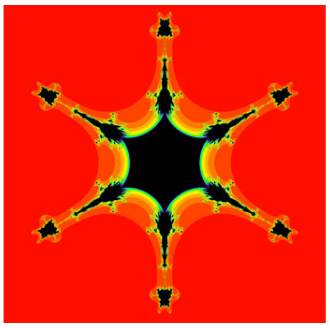

FIGURE 22. Multicorn generated via PMO for $\theta = 0.05$ and $k = 5$.

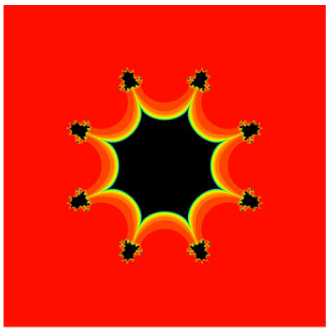

FIGURE 23. Multicorn generated via PMO for $\theta = 0.2$ and $k = 7$.

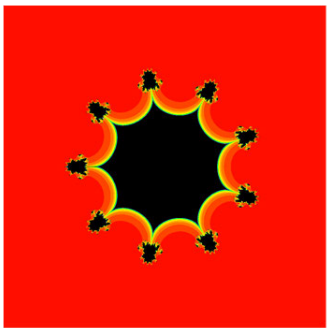

FIGURE 24. Multicorn generated via PMO for $\theta = 0.4$ and $k = 8$.

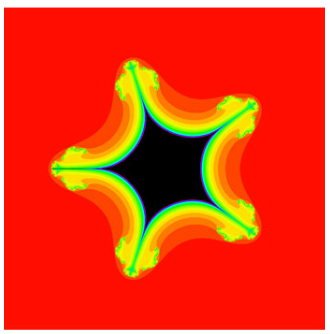

FIGURE 25. Multicorn generated via MO for $\theta = 0.5$ and $k = 4$.

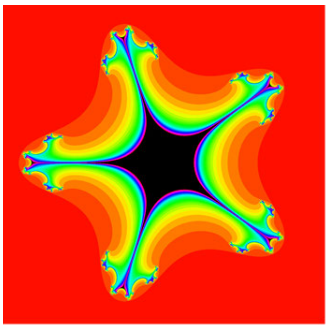

FIGURE 26. Multicorn generated via MO for $\theta = 0.07$ and $k = 4$.

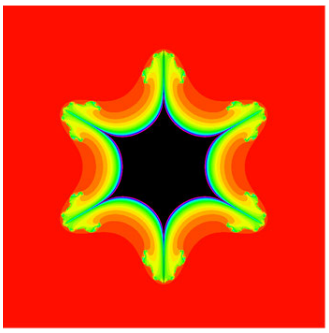

FIGURE 27. Multicorn generated via MO for $\theta = 0.3$ and $k = 5$.

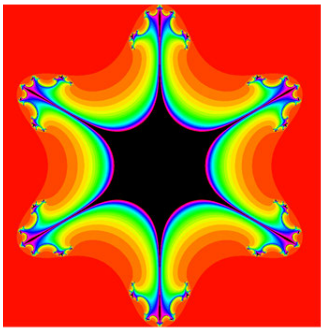

FIGURE 28. Multicorn generated via MO for $\theta = 0.05$ and $k = 5$.

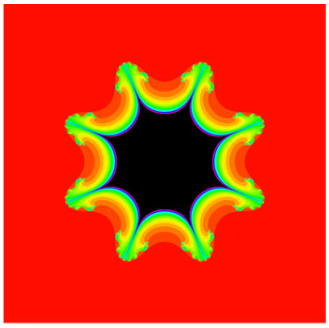

FIGURE 29. Multicorn generated via MO for $\theta = 0.2$ and $k = 7$.

of multicorn is around both x-axis and y-axis. Also multicorns maintain $(k + 1)$-fold rotational symmetries. Tricorns and multicorns generated in PMO are quite different from those generated in MO for similar value of θ (see Figs. 2 and 6, Figs. 3 and 7, Figs. 11 and 15, Figs. 12 and 16 etc). Patterns generated in PMO are more clear than those generated in MO

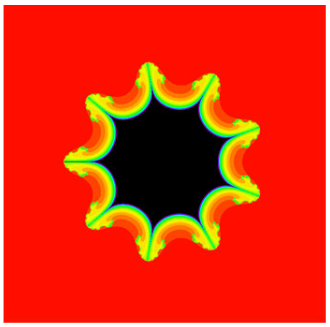

FIGURE 30. Multicorn generated via MO for $\theta = 0.4$ and $k = 8$.

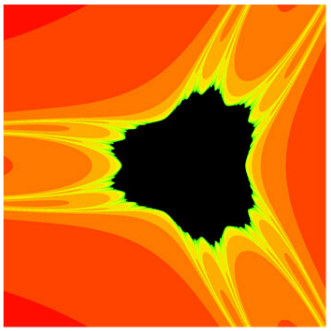

FIGURE 31. Anti-Julia set generated via PMO.

and interesting changes are seen in the figures for various values of θ.

D. ANTI-JULIA SETS FOR QUADRATIC FUNCTION

In Figs. 31–35 anti-Julia sets for $Q_c(\bar{z}) = \bar{z}^2 + c$ are presented in PMO and in Figs. 36–40 anti-Julia sets are visualized in MO. The usual parameters used to generate the images are the following:

- In Fig. 31 with $A = [-3.5, 2.5] \times [-3.0, 3.0]$ anti-Julia set is displayed in PMO and in Fig. 36 with $A = [-20, 12] \times [-16, 16]$ anti-Julia set is visualized in MO for similar value of $c = 0.001 + 0.005\mathbf{i}$ and $\theta = 0.1$.
- In Fig. 32 with $A = [-5.5, 2.5] \times [-4.0, 4.0]$ while in Fig. 37 with $A = [-7.5, 4.5] \times [-6.0, 6.0]$ anti-Julia sets are presented via PMO and MO respectively for same value of $c = 0.001 + 0.005\mathbf{i}$ and $\theta = 0.3$.
- In Fig. 33 and in Fig. 38 with $A = [-3.5, 2.5] \times [-3.0, 3.0]$ for same value of $c = 0.03 - 0.02\mathbf{i}$ and $\theta = 0.5$ anti-Julia sets are presented via PMO and MO respectively.
- In Fig. 34 with $A = [-6.1, 4.3] \times [-5.2, 5.2]$ anti-Julia set is presented in PMO and in Fig. 39 with $A = [-10.0, 6.0] \times [-8.0, 8.0]$ anti-Julia set is visualized in MO for similar value of $c = 0.001 + 0.005\mathbf{i}$ and $\theta = 0.2$.
- In Fig. 35 with $A = [-3.5, 2.5] \times [-3.0, 3.0]$ anti-Julia sets is visualized in PMO and in Fig. 40 with $A = [-35, 25] \times [-30, 30]$ anti-Julia set is presented in MO for the same value of $\theta = 0.06$ and $c = 0.023 - 0.35\mathbf{i}$.

FIGURE 32. Anti-Julia set generated via PMO.

FIGURE 33. Anti-Julia set generated via PMO.

FIGURE 34. Anti-Julia set generated via PMO.

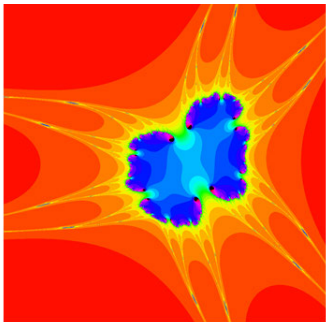

FIGURE 35. Anti-Julia set generated via PMO.

E. ANTI-JULIA SETS FOR CUBIC FUNCTION

In Figs. 41–45 anti-Julia sets for the function $Q_c(\bar{z}) = \bar{z}^3 + c$ are presented in PMO and in Figs. 46–50 anti-Julia sets are

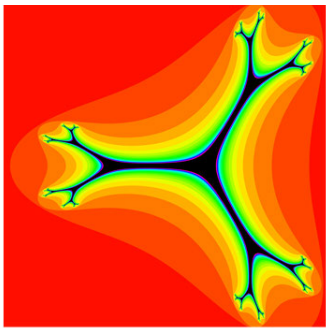

FIGURE 36. Anti-Julia set generated via MO.

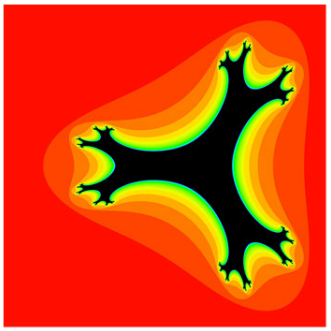

FIGURE 37. Anti-Julia set generated via MO.

FIGURE 38. Anti-Julia set generated via MO.

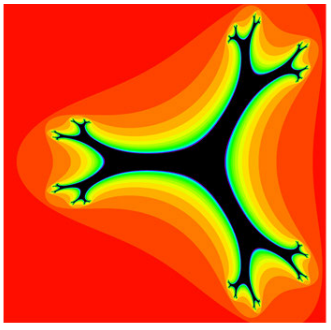

FIGURE 39. Anti-Julia set generated via MO.

displayed in MO. The usual parameters used to generate the images are: $K = 30$ and $A = [-2.5, 2.5] \times [-2.5, 2.5]$. Whereas, the varying parameters are the following:

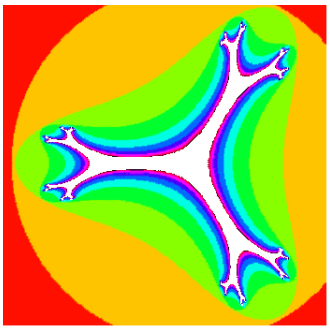

FIGURE 40. Anti-Julia set generated via MO.

FIGURE 41. Anti-Julia set generated via PMO for $\theta = 0.3$ and $c = 0.001 + 0.005\mathbf{i}$.

FIGURE 42. Anti-Julia set generated via PMO for $\theta = 0.5$ and $c = 0.001 + 0.005\mathbf{i}$.

- In Fig. 41 anti-Julia set in PMO and in Fig. 46 anti-Julia set in MO are presented for similar value of $\theta = 0.3$ and $c = 0.001 + 0.005\mathbf{i}$.
- In Fig. 42 anti-Julia set in PMO while anti-Julia set in MO visualized in Fig. 47 for same value of $\theta = 0.5$ and $c = 0.001 + 0.005\mathbf{i}$.
- Anti-Julia sets visualized in Fig. 43 and Fig. 48 via PMO and MO for $\theta = 0.2$ and $c = -0.25\mathbf{i}$.
- Anti-Julia sets presented in Fig. 44 and Fig. 49 in PMO and MO for same value of $\theta = 0.4$ and $c = -0.25\mathbf{i}$.
- Anti-Julia sets displayed in Fig. 45 and Fig. 50 in PMO and MO respectively for same value of $\theta = 0.5$ and $c = -0.25\mathbf{i}$.

We observed that connected anti-Julia sets generated for quadratic function via PMO maintain symmetry along x-axis

FIGURE 43. Anti-Julia set generated via PMO for $\theta = 0.2$ and $c = -0.25i$.

FIGURE 44. Anti-Julia set generated via PMO for $\theta = 0.4$ and $c = -0.25i$.

FIGURE 45. Anti-Julia set generated via PMO for $\theta = 0.5$ and $c = -0.25i$.

FIGURE 46. Anti-Julia set generated via MO for $\theta = 0.3$ and $c = 0.001 + 0.005i$.

FIGURE 47. Anti-Julia set generated via MO for $\theta = 0.5$ and $c = 0.001 + 0.005i$.

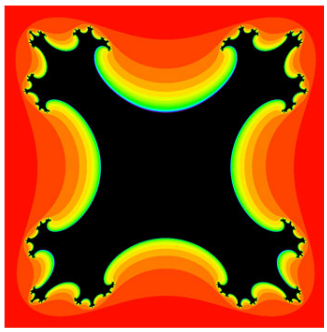

FIGURE 48. Anti-Julia set generated via MO for $\theta = 0.2$ and $c = -0.25i$.

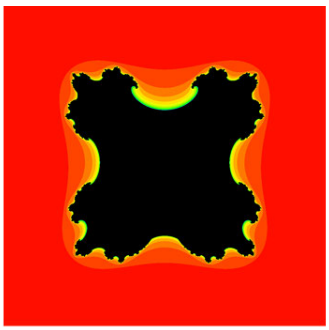

FIGURE 49. Anti-Julia set generated via MO for $\theta = 0.4$ and $c = -0.25i$.

FIGURE 50. Anti-Julia set generated via MO for $\theta = 0.5$ and $c = -0.25i$.

while anti-Julia sets for cubic function preserve symmetry around both x-axis and y-axis. Anti-Julia sets generated in PMO are entirely different from those generated in MO for similar values of θ and c (see Figs. 31 and 36, Figs. 32 and 37, Figs. 33 and 38, Figs. 34 and 39, Figs. 41 and 46, Figs. 42 and 47 etc).

IV. CONCLUSION

In the present paper we introduced and visualized antifractals in hybrid PMO and compare it with antifractals generated in MO. Escape criterion for antifractals has been established corresponding to PMO and visualized the pattern of tricorns, multicorns and anti-Julia sets. In the dynamics of antipolynomials $z \to \bar{z}^k + c$ for $k \geq 2$, we obtained various patterns of tricorns and multicorns for the same value of k and choosing different values of θ in PMO. We observed that the number of branches attached to the main body of the tricorns and multicorns are $k + 1$ and many branches have subbranches. We also found that the symmetry of multicorn is about both x-axis and y-axis when k is odd but for k is even the symmetry is preserved only along x-axis. A few examples of connected anti-Julia sets have been presented for quadratic and cubic functions. Interesting changes are seen in the figures for different values of parameter θ. Tricorn prints are utilized commercially such as tricorn mugs and tricorn dresses like tricorn T-shirts. We think that results of this paper will impress those who are interesting in creating automatically aesthetic patterns.

REFERENCES

[1] A. Hundertmark-Zaušková, "On the convergence of fixed point iterations for the moving geometry in a fluid-structure interaction problem," *J. Differ. Equ.*, vol. 267, no. 12, pp. 7002–7046, Dec. 2019.
[2] S. H. Strogatz, *Nonlinear Dynamics And Chaos: With Applications to Physics, Biology, Chemistry, And Engineering*. Boca Raton, FL, USA: CRC Press, 2018.
[3] G. Julia, "Memoire sur l'iteration des fonctions rationnelles," *J. Math. Pures Appl.*, vol. 8, pp. 245–247, 1918.
[4] M. F. Barnsley, *Fractals Everywhere*. New York, NY, USA: Academic, 2014.
[5] S. Mukherjee, S. Nakane, and D. Schleicher, "On multicorns and unicorns II: Bifurcations in spaces of antiholomorphic polynomials," *Ergodic Theory Dyn. Syst.*, vol. 37, no. 3, pp. 859–899, May 2017.
[6] B. B. Mandelbrot, *The Fractal Geometry of Nature*, vol. 2. New York, NY, USA: Freeman, 1982.
[7] R. Devaney, *A First Course In Chaotic Dynamical Systems: Theory And Experiment*. New York, NY, USA: Addison-Wesley, 1992.
[8] E. B. Burger and M. Starbird, *The Heart of Mathematics: An Invitation to Effective Thinking*. Springer, 2004.
[9] S. R. Holtzman, *Digital Mantras: The Languages of Abstract and Virtual Worlds*. Cambridge, MA, USA: MIT Press, 1995.
[10] S. Kang, A. Rafiq, A. Latif, A. Shahid, and F. Alif, "Fractals through modified iteration scheme," *Filomat*, vol. 30, no. 11, pp. 3033–3046, 2016.
[11] Ashish, M. Rani, and R. Chugh, "Julia sets and mandelbrot sets in noor orbit," *Appl. Math. Comput.*, vol. 228, pp. 615–631, Feb. 2014.
[12] S. Y. Cho, A. A. Shahid, W. Nazeer, and S. M. Kang, "Fixed point results for fractal generation in noor orbit and s-convexity," *SpringerPlus*, vol. 5, no. 1, p. 1843, Dec. 2016.
[13] Y. C. Kwun, A. A. Shahid, W. Nazeer, M. Abbas, and S. M. Kang, "Fractal generation via CR iteration scheme with s-convexity," *IEEE Access*, vol. 7, pp. 69986–69997, 2019.
[14] C. Zou, A. A. Shahid, A. Tassaddiq, A. Khan, and M. Ahmad, "Mandelbrot sets and julia sets in picard-mann orbit," *IEEE Access*, vol. 8, pp. 64411–64421, 2020.
[15] K. Mitchell, "The fractal art manifesto," Disponível, Tech. Rep., 1999. [Online]. Available: http://www.kerrymitchellart.com/articles/manifesto/fa-manifesto.html
[16] W. D. Crowe, R. Hasson, P. J. Rippon, and P. E. D. Strain-Clark, "On the structure of the mandelbar set," *Nonlinearity*, vol. 2, no. 4, pp. 541–553, Nov. 1989.
[17] J. W. Milnor, "Dynamics in one complex variable: Introductory lectures," 1990, *arXiv:math/9201272*. [Online]. Available: https://arxiv.org/abs/math/9201272
[18] R. Winters, "Bifurcations in families of antiholomorphic and biquadratic maps," Ph.D. dissertation, Dept. Math., Boston Univ., Boston, MA, USA, 1990.
[19] E. Lau and D. Schleicher, "Symmetries of fractals revisited," *Math. Intelligencer*, vol. 18, no. 1, pp. 45–51, Dec. 1996.
[20] S. Nakane and D. Schleicher, "On multicorns and unicorns I: Antiholomorphic dynamics, hyperbolic components and real cubic polynomials," *Int. J. Bifurcation Chaos*, vol. 13, no. 10, pp. 2825–2844, Oct. 2003.
[21] R. L. Devaney, *A First Course In Chaotic Dynamical Systems: Theory And Experiment*. Boca Raton, FL, USA: CRC Press, 2018.
[22] W. R. Mann, "Mean value methods in iteration," *Proc. Amer. Math. Soc.*, vol. 4, no. 3, p. 506, Mar. 1953.
[23] M. Rani, "Superior antifractals," in *Proc. 2nd Int. Conf. Comput. Autom. Eng. (ICCAE)*, Feb. 2010, pp. 798–802.
[24] M. Rani, "Superior tricorns and multicorns," in *Proc. 9th WSEAS Int. Conf. Appl. Comput. Eng.* Athens, Greece: World Scientific and Engineering Academy and Society (WSEAS), 2010, pp. 58–61.
[25] Y. S. Chauhan, R. Rana, and A. Negi, "New tricorn and multicorns of Ishikawa iterates," *Int. J. Comput. Appl.*, vol. 7, no. 13, pp. 25–33, 2010.
[26] M. Rani and R. Chugh, "Dynamics of antifractals in noor orbit," *Int. J. Comput. Appl.*, vol. 57, no. 4, pp. 11–15, Jan. 2012.
[27] N. Partap, S. Jain, and R. Chugh, "Computation of antifractals-tricorns and multicorns and their complex nature," *Pertanika J. Sci. Technol.*, vol. 26, no. 2, pp. 863–872, 2018.
[28] S. Ishikawa, "Fixed points by a new iteration method," *Proc. Amer. Math. Soc.*, vol. 44, no. 1, p. 147, Jan. 1974.
[29] Y. C. Kwun, A. A. Shahid, W. Nazeer, S. I. Butt, M. Abbas, and S. M. Kang, "Tricorns and multicorns in noor orbit with s-convexity," *IEEE Access*, vol. 7, pp. 95297–95304, 2019.
[30] Z. Chen, A. A. Shahid, T. J. Zia, I. Ahmed, and W. Nazeer, "Dynamics of antifractals in modified *S*-iteration orbit," *IEEE Access*, vol. 7, pp. 113114–113120, 2019.
[31] S. M. Kang, A. Rafiq, A. Latif, A. A. Shahid, and Y. C. Kwun, "Tricorns and multicorns of S-iteration scheme," *J. Function Spaces*, vol. 2015, pp. 1–7, Jan. 2015.
[32] R. Agarwal, D. O. Regan, and D. Sahu, "Iterative construction of fixed points of nearly asymptotically nonexpansive mappings," *J. Nonlinear Convex Anal.*, vol. 8, no. 1, p. 61, 2007.
[33] D. Li, A. A. Shahid, A. Tassaddiq, A. Khan, X. Guo, and M. Ahmad, "CR iteration in generation of antifractals with s-convexity," *IEEE Access*, vol. 8, pp. 61621–61630, 2020.
[34] S. H. Khan, "A Picard-Mann hybrid iterative process," *Fixed Point Theory Appl.*, vol. 2013, no. 1, p. 69, Dec. 2013.

WEI WANG was born in Shijiazhuang, Hebei, China, in 1986. He received the bachelor's and master's degrees from NUDT, China, in 2005 and 2013, respectively. He is currently pursuing the degree with the College of Automation Science and Electrical Engineering, Beihang University. His research interests include computational intelligence, machine learning, information security, and big data analysis.

XIAOHUI HU was born in China, in 1960. He received the Ph.D. degree in computer science from Beihang University, China, in 2003. He is currently a Professor with the Institute of Software, Chinese Academy of Sciences. His research interests include big data, deep learning, and computer vision.

ABDUL AZIZ SHAHID received the M.Phil. degree in mathematics from Lahore Leads University, Lahore, Pakistan, in 2014. He is currently a Ph.D. Research Scholar with The University of Lahore, Lahore. He has published over 15 research articles in different international journals. His research interests include fixed point theory and fractal generation via different fixed point iterative schemes.

MINGYE WANG was born in China, in 1992. He is currently pursuing the Ph.D. degree with Beihang University, with major of pattern recognition and intelligent systems. His main research interests include deep learning and computer vision.